

See discussions, stats, and author profiles for this publication at: <https://www.researchgate.net/publication/215827420>

# Simultaneous Quantification of Multiple Nucleic Acid Targets Using Chemiluminescent Probes

ARTICLE *in* JOURNAL OF THE AMERICAN CHEMICAL SOCIETY · SEPTEMBER 2011

Impact Factor: 12.11 · DOI: 10.1021/ja202221h · Source: PubMed

---

CITATIONS

16

---

READS

46

5 AUTHORS, INCLUDING:



**Kenneth A Browne**

GIMDx, Inc.

26 PUBLICATIONS 815 CITATIONS

SEE PROFILE



**Dimitri D Deheyn**

University of California, San Diego

78 PUBLICATIONS 676 CITATIONS

SEE PROFILE



**Gamal A El-Hiti**

King Saud University

210 PUBLICATIONS 1,389 CITATIONS

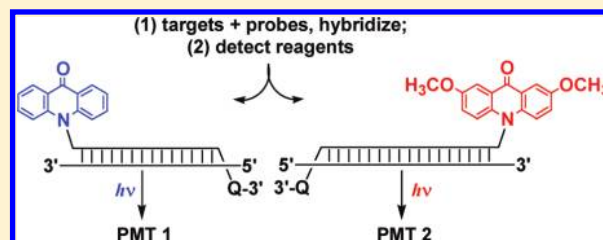
SEE PROFILE

## Simultaneous Quantification of Multiple Nucleic Acid Targets Using Chemiluminescent Probes

Kenneth A. Browne,<sup>\*,†</sup> Dimitri D. Deheyn,<sup>‡</sup> Gamal A. El-Hiti,<sup>§</sup> Keith Smith,<sup>§</sup> and Ian Weeks<sup>||,⊥</sup><sup>†</sup>Gen-Probe Incorporated, 10210 Genetic Center Drive, San Diego, California 92121, United States<sup>‡</sup>Marine Biology Research Division, Scripps Institution of Oceanography, University of California at San Diego, La Jolla, California 92093, United States<sup>§</sup>School of Chemistry, Cardiff University, Main Building, Park Place, Cardiff, Wales CF10 3AT, U.K.<sup>||</sup>Molecular Light Technology Research Limited (now Gen-Probe Cardiff Ltd.), 5 Chiltern Close, Cardiff Industrial Park, Cardiff, Wales CF14 5DL, U.K.

## S Supporting Information

**ABSTRACT:** A novel method is described for simultaneous detection and quantification of attomoles or a few femtomoles of two (or potentially more) nucleic acid targets, without need for amplification. The technique depends on spectral–temporal resolution of chemiluminescence emitted from independent hybridization-induced chemiluminescent signal probes. The probes are internally quenched except in the presence of their specific targets, thereby allowing detection limits up to 10 000 times lower than with fluorescent probes. This is sufficient to obviate the need for amplification in many cases. The utility of the technique has been demonstrated by use of resolvable N-linked acridinium and 2,7-dimethoxyacridinium ester labeled probes in a homogeneous assay for sensitive and simultaneous independent quantification of pan-bacterial and pan-fungal target sequences in seawater.



## INTRODUCTION

The presence of important and potentially pathogenic viral, bacterial, fungal, eukaryotic, or other species in dietary, agricultural, pharmaceutical, forensic, clinical, and environmental specimens requires rapid and sensitive methods for both identification and quantification of such organisms. In this context, molecular detection techniques such as sequencing,<sup>1</sup> microarrays,<sup>2</sup> and nucleic acid probes<sup>3</sup> are becoming increasingly important. For rapid time-to-result, sensitivity and specificity, probes are especially useful, but in order for them to be effective tools, target-bound probes need to be distinguished from probes that are not bound to target. This may be accomplished by separating bound from unbound probes (heterogeneous methods, as commonly carried out with radioisotopically labeled probes), then querying the bound fraction for the detectable signal. However, such methods increase the complexity of an assay and also provide opportunities for contamination with probes and/or target analytes in the reaction vessel.

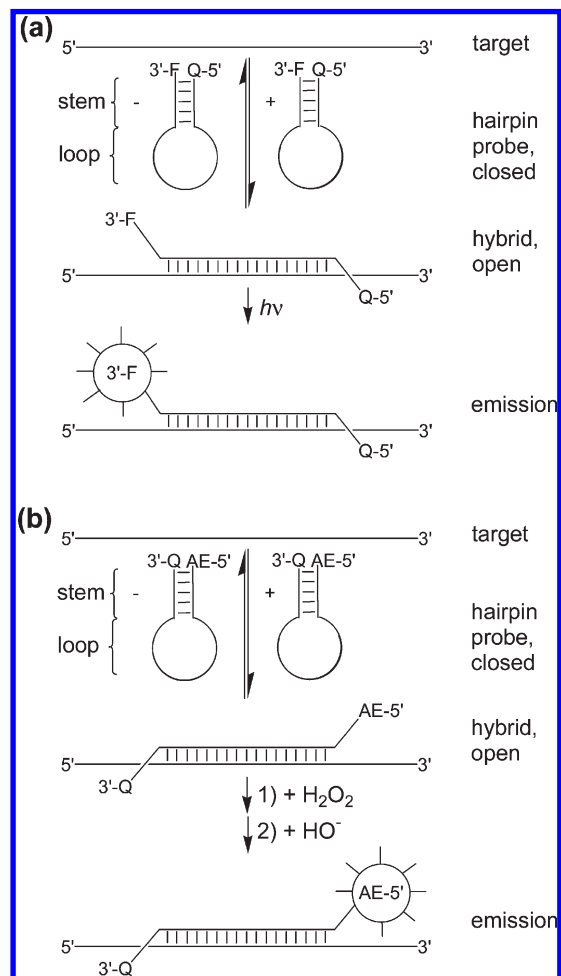
Methods that avoid undue handling such as separations are favored. For example, self-reporting nucleic acid probes labeled with interacting fluorophore and quenching moieties (e.g., molecular beacons (MBs),<sup>3a</sup> hairpin inversion probes,<sup>4</sup> molecular torches<sup>5</sup>) are powerful tools for analytical or diagnostic detection of nucleic acid targets. In the case of MBs (Scheme 1a), fluorescence induced by photoexcitation is lower in the absence of target and increases as binding to

complementary nucleic acids induces increased distance between fluorophore and quenching moieties. Excess unbound probe exhibits lower emission than bound probe, and so separation is unnecessary, supporting a homogeneous assay format. Furthermore, careful selection of narrow band excitation sources or filters coupled with appropriate emission filters advantageously supports the simultaneous discrimination of two or more differently labeled fluorescent probes and, hence, can indicate the presence or absence of multiple analyte nucleic acids in a single assay. However, despite mitigating instrumentation and procedural designs, organic fluorescent probes tend to have a high background relative to the emitted signal caused by using a light source to initiate light emission phenomena, incomplete quenching, and the intrinsic photofluorescence of many species present in biological samples, including nucleic acids themselves. This means that the relationship between luminescence intensity and target nucleic acid concentration is not linear where the background contribution to the overall signal is significant and, thus, limits signal-based detection typically to nanomolar concentrations. Since organisms of interest may be present in low abundance, fluorescent probe-based detection often requires high yield target amplification methods

Received: March 10, 2011

Published: July 25, 2011

**Scheme 1. Comparison of Interactions and Excitations/Emissions of Self-Quenching (a) Fluorescent or (b) Chemiluminescent Hairpin Probes (MBs and HICS Probes, Respectively) with Complementary Target Nucleic Acids<sup>a</sup>**



<sup>a</sup> Solid lines between nucleic acid strands represent base pairing. F and Q represent fluorophore and quencher moieties, respectively. AE is an acridinium ester chemiluminescent moiety.

such as the polymerase chain reaction (PCR)<sup>6</sup> or transcription-mediated amplification (TMA);<sup>7</sup> however, amplification necessarily increases the complexity, time, and expense of the assay. Although time-to-detectable result can be improved by so-called real-time-amplification procedures in which fluorescent probes are monitored during amplification, it would still be advantageous to avoid amplification altogether.

By definition, emissions from chemiluminescent probes are the result of one or more chemical reactions. Since their detection is by observation without stimulation (e.g., excitation light), such probes are necessarily not perturbed by the interrogation technique. Therefore, unlike fluorescent probes, emission responses from chemiluminescent probes benefit from much lower intrinsic background emission so that such probes can be extremely sensitive and also offer a linear relationship between the magnitude of luminescence and the quantity of target nucleic acid present in specimens at low concentrations. Acridinium ester (AE) chemiluminescent nucleic acid probes have traditionally had the AE moiety linked through the C9

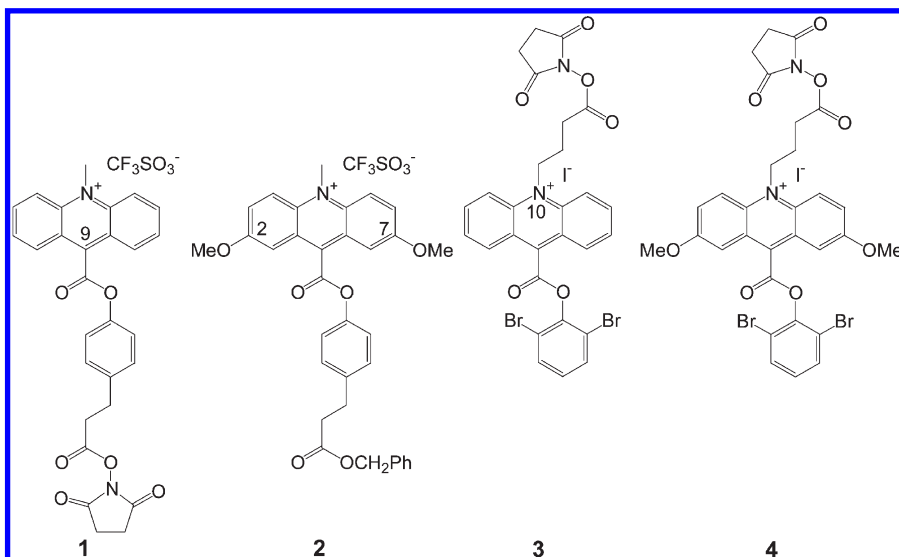
acridinium position (C-linked) via an aminoalkyl group to a linear oligonucleotide containing 18–30 nucleotide (nt) units.<sup>8</sup> After the probe has hybridized to its complementary target, bound and nonbound AE probes could be physically separated, allowing detection of signal from only bound AE probe (in a heterogeneous assay). Alternatively, bound and nonbound AE probes have been differentiated by mild alkaline treatment in which the ester moiety of the nonbound AE probe is selectively hydrolyzed, rendering these probes nonchemiluminescent, while the ester of the AE probe hybridized to complementary target is protected from hydrolysis by its interaction with the nucleic acid double strands; this is the basis of the homogeneous hybridization protection assay.<sup>8</sup> AE probe detection is initiated chemically by addition of hydrogen peroxide ( $H_2O_2$ ) followed by a concentrated base solution, which leads to highly luminescent emissions from the released, excited *N*-methylacridone. The signals are typically detected with a very sensitive photomultiplier tube (PMT) that sums photons from across the entire *N*-methylacridone emission spectrum (while typically reported as 430 nm,<sup>8</sup> these emissions actually range from ~400 to 540 nm). This leads to a detection limit of ~600 fM (about  $10^3$ - to  $10^4$ -fold more sensitive than typical fluorescent probes) and a quantitative dynamic range spanning ~4 orders of magnitude.<sup>8</sup> Such high sensitivity supports either direct detection of nucleic acid analytes or detection of amplified analytes after only limited amplification.

Recently, a new probe type, the hybridization-induced chemiluminescent signal (HICS) probe, has been developed.<sup>9,10</sup> HICS probes comprise an AE moiety conjugated through the N10 acridinium position (N-linked) to a site near one terminus of a stem-loop oligonucleotide and a quenching moiety attached near the opposite terminus (Scheme 1b), therefore resembling fluorescent MBs (Scheme 1a). Similar to MBs, upon hybridization of the HICS probe loop region to a complementary target nucleic acid, the stem dissociates, distancing the chemiluminescent moiety from the quencher and allowing light emission to be detected upon chemical initiation. Thus, HICS probes self-report upon binding complementary nucleic acids, and probes in excess of target do not require physical or chemical separation from hybridized probes, allowing use in a homogeneous assay. Unlike with their fluorescent counterparts, however, since no methods are available for simultaneous and independent determination of the emissions from different probes, quantitative use of HICS probes has been limited to measurement of only one analyte in each assay. To overcome this limitation, some novel developments are required: (i) synthesis of two or more different emitter moieties that can be independently detected, for example, as a result of differences in wavelengths or kinetics of emission; (ii) adaptation of a typical luminometer to allow it to differentiate the emissions from the different emitters; (iii) development of a protocol for carrying out multiple analyte detection. Here, we report development of such a system and demonstrate its utility by independently measuring amounts of a pan-fungal nucleic acid sequence and a pan-bacterial nucleic acid sequence in seawater simultaneously, in a single assay, without need for amplification.

## RESULTS AND DISCUSSION

**Probe Design.** In order to allow detection of two nucleic acid analytes using pairs of HICS probes, the two probes must differ both in their ability to recognize different oligonucleotide

Chart 1. Comparison of acridinium ester reagent structures



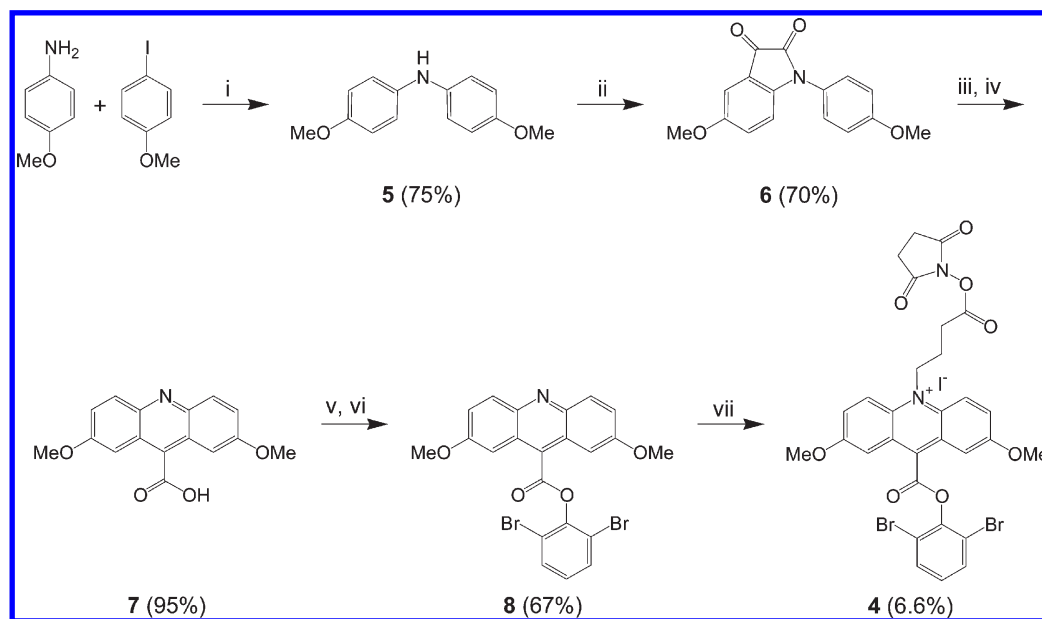
sequences and in the nature of the luminescence they emit. Each probe molecule must incorporate four features: (i) an oligonucleotide strand complementary to an oligonucleotide sequence in a particular target nucleic acid marker; (ii) extensions on either side of the aforesaid oligonucleotide sequence by oligonucleotide strands (stem arms) complementary to each other so that they cause the two ends of the oligonucleotide to bind to each other in a hairpin-like arrangement; (iii) a chemiluminophore unit attached to one end of the oligonucleotide sequence via an aminoalkyl group or related spacer; (iv) a quencher for the luminescence emitted by the chemiluminophore, attached to the other end of the oligonucleotide sequence via an appropriate spacer (see Scheme 1). The stem arms may be partially or completely complementary to the target sequence. When the stem arms hybridize to themselves in the absence of target, the target complementary sequence typically forms a loop structure. The starting point was to design an appropriate pair of reagents to introduce two differentiable chemiluminophores.

*Design of Chemiluminophores for Incorporation into the Probes.* 9-(4-(2-Succinimidyl-ethoxy-carbonyl)phenoxy-carbonyl)-10-methylacridinium trifluoromethanesulfonate (**1**, Chart 1) is an unsubstituted AE labeling reagent that has been used to generate biological probes having C-linked AE moieties.<sup>11</sup> It comprises (i) an active group (*N*-hydroxysuccinimide, NHS) capable of ready attachment to an amino substituent in the unlabeled probe, (ii) a leaving group (the substituted phenoxide) that is eliminated during treatment with alkaline  $\text{H}_2\text{O}_2$ , and (iii) a chemiluminescent group (the AE unit, which is converted into excited state *N*-methylacridone during treatment with alkaline  $\text{H}_2\text{O}_2$ ). Substituents on the phenoxy group primarily influence the rate of the chemiluminescent reaction, while those on the acridine unit have a major influence on the wavelength of emission. We investigated one design pathway, wavelength-resolvable AE probes, in our attempt to develop appropriate systems. This required a substituted AE that emitted luminescence distinct from that characteristic of compound **1**.

While physicochemical rationalization can assist in the design of longer wavelength-emitting *N*-alkylacridone precursors, empirical studies are required to discover AE derivatives that balance the increased emission wavelength (e.g.,  $\geq 50$  nm) needed to distinguish them from the unsubstituted AE in aqueous solution

with stability in aqueous environments and the ability to initiate chemiluminescence under conditions that will not damage oligonucleotide hybrids. Woodhead et al. posited that extending the conjugation of the acridinium ring system to a 2,4-pentadienoic acid moiety would reduce the energy gap between the excited and ground state *N*-methylacridone species, resulting in a bathochromic shift of chemiluminescent emission wavelength by up to 80 nm compared to an unmodified AE.<sup>12</sup> However, Law et al. later synthesized a closely related AE and found only a 37 nm increase in peak emission wavelength in an acetonitrile solution.<sup>13</sup> Law et al. also extended their studies to include AEs fused to additional aromatic rings and reported that the excited *N*-methylbenzacridone from the angular benz[*a*]acridinium ester derivative increased peak emission by only 11 nm while the excited *N*-methylbenzacridone from the linear benz[*b*]AE derivative increased peak emission wavelength by 95 nm in acetonitrile solutions.<sup>13</sup> In a series of *N*-sulfopropyl AEs, Natrajan et al. reported that incorporation of a single methoxy group at the acridinium ring 3 position led to a slight (8 nm) hypsochromic shift in the maximum emission wavelength whereas incorporation of the substituent at the 2 or 4 position led to increases in the peak emission wavelength of 32 and 52 nm, respectively.<sup>14</sup> They also found that 2,7-dimethoxy substitution of their *N*-sulfopropyl AE led to a 58 nm increase in the maximum emission wavelength.<sup>14</sup>

We have previously synthesized a considerable variety of AEs with different substituents on both the phenoxide and acridine rings.<sup>15</sup> In the course of those studies, we sometimes observed that, relative to an unmodified AE, the changes in peak chemiluminescent wavelengths on introduction of a particular substituent are not always the same as the changes reported in the literature for similar systems. Effects of different solvents used may account for at least part of the differences in observed photonic behaviors. However, we did observe that the emission wavelength of 2,7-dimethoxy-9-(4-benzoyloxycarbonyl-ethylphenoxy-carbonyl)-10-methylacridinium trifluoromethanesulfonate (**2**, Chart 1) was 55 nm longer than that from reagent **1** in aqueous solution, presumably because of electron donation (+I) from the two methoxy groups.<sup>15e</sup>

Scheme 2. Synthesis of N-Linked 2,7-DimethoxyAE NHS Ester Label (4)<sup>a</sup>

<sup>a</sup> Reagents and conditions: (i) CuI, K<sub>2</sub>CO<sub>3</sub>, L-proline, DMSO, 48 h, 90 °C; (ii) (ClCO)<sub>2</sub>, AlCl<sub>3</sub>, HCl; (iii) aq KOH, 72 h; (iv) HCl; (v) SOCl<sub>2</sub>; (vi) 2,6-dibromophenol; (vii) succinimidyl 4-iodobutanoate, 3 h, 150 °C.

9-(2,6-Dibromophenoxy)carbonyl-10-(3-succinimidylloxycarbonylpropyl)acridinium iodide labeling reagent **3** was used to produce previously reported HICS probes.<sup>10</sup> It incorporates two features that differ significantly from labeling reagent **1**. First, it results in N-linked attachment of the AE label to oligonucleotides rather than through the phenolic leaving group. When chemically initiated, light from these probes is emitted from an excited *N*-alkylacridone species that remains linked to the oligonucleotide. In the absence of target, the stem forces the emitter and the quencher to remain proximal and, hence, allows little energy to be emitted as detectable light upon initiation. Second, the bulky, electron-withdrawing (−I) bromo substituents help protect the ester from facile hydrolysis and also decrease the p*K*<sub>a</sub> of the leaving group phenol, thereby supporting formation of the excited *N*-alkylacridone under mildly alkaline conditions that maintain nucleic acid hybrids. We selected this reagent for labeling our unsubstituted AE probes and the 2,7-dimethoxy analogue (**4**, Chart 1) for labeling the differentiable probes.

**Syntheses of Reagents 3 and 4.** Compound **3** was obtained by a published procedure.<sup>10</sup> The preparation of compound **4** followed a similar route but with additional steps to produce 2,7-dimethoxyacridine-9-carboxylic acid (**7**) prior to esterification and quaternization (Scheme 2). Bis(4-methoxyphenyl)amine (**5**) was prepared in 75% yield according to a standard literature procedure.<sup>16</sup> Reaction of compound **5** with oxalyl chloride in dichloromethane followed by treatment with aluminum chloride gave *N*-(4-methoxyphenyl)-5-methoxyisatin (**6**) in 70% yield, which on treatment with potassium hydroxide under reflux conditions for 72 h gave 2,7-dimethoxyacridine-9-carboxylic acid (**7**) in 95% yield. A mixture of compound **7** and freshly redistilled thionyl chloride was heated under reflux for 3 h to afford the corresponding acid chloride, which on reaction with 2,6-dibromophenol in pyridine at 70 °C gave 2,6-dibromophenyl 2,7-dimethoxyacridine-9-carboxylate (**8**) in 67% yield. Reaction of compound **8** with succinimidyl 4-iodobutanoate at 150 °C for

3 h gave 2,7-dimethoxy-9-(2,6-dibromophenoxy)acridinium iodide (**4**) in 6.6% yield. The low yield resulted from a very slow reaction, even at 150 °C. Use of even more forcing conditions caused some decomposition of the starting material, whereas under the conditions reported most of the unreacted starting material could be recovered without detectable side products. Thus, all except the last step gave reasonable yields. An even lower yield was reported in the final step of the published synthesis of compound **3**.<sup>10</sup>

**Selection and Synthesis of Targets.** Four target sequences were selected (Table 1) as representatives of two different, broad microbial groups found in environmental samples such as seawater (*Escherichia coli* and *Candida albicans*)<sup>17</sup> or of two pathogens that may occur individually or simultaneously in human urogenital swab or urine specimens (*Chlamydia trachomatis* and *Neisseria gonorrhoeae*).<sup>18</sup> In order to mimic more closely the natural nucleic acid materials, the synthetic target oligonucleotide sequences exceeded the length of the part (central in each target in Table 1) for which complementary sequences in probes would be constructed. These targets were synthesized on automated oligonucleotide synthesizers by established methods using phosphoramidite monomers, then purified and quantified prior to use. With the targets available, the next stage was to generate appropriate oligonucleotide strands for the probes.

**Design and Synthesis of Probe Oligonucleotide Sequences.** HICS probe sequences (Table 1) were based on earlier fluorescent probes<sup>4</sup> used in detection of pan-bacterial and pan-fungal species or were derived from earlier probe sequences<sup>19</sup> used to detect *Ctr* and *Ngo* specifically but with self-complementary arm sequences added to each pair of termini. The probes were also synthesized on automated oligonucleotide synthesizers by established methods using phosphoramidite monomers. Several different pairs of stem arms were incorporated into the oligonucleotide sequences, all of which included GC clamps at



Table 1. Nucleic Acid Sequences for Chosen Targets and the Probes Developed for Them

name <sup>a</sup>	nucleic acid backbone <sup>b,c</sup>	sequence <sup>c</sup> and substituents <sup>d</sup>
<i>EcoB1932-1947(-)</i> HICS16	DNA/OMe	5'-AE- <u>GGCTCCTG</u> CGACAAGGAAUUUCGC <u>CAGGAGCC</u> -MR-3'
<i>EcoB1932-1947(-)</i> HICS17	DNA/OMe	5'-AE- <u>CCGAGGAC</u> CGACAAGGAAUUUCGC <u>GTCTCTCGG</u> -BHQ2-3'
<i>EcoB1932-1947(-)</i> HICS18	DNA/OMe	5'-AE- <u>CCCAGCAC</u> CGACAAGGAAUUUCGC <u>GTGCTGGG</u> -BHQ2-3'
<i>EcoB1921-1958(+)</i>	RNA	3'-GCCUUGAAUGG GCUGUCCUUAAGCG AUGGAAUCCUG-5'
		<div style="display: flex; justify-content: space-around; width: 100%;"> <span> </span> <span> </span> <span> </span> </div> <div style="display: flex; justify-content: space-around; width: 100%;"> <span>1950</span> <span>1940</span> <span>1930</span> </div>
<i>CalA1185-1206(-)</i> HICS86	DNA	5'-AE- <u>GGCTCCTG</u> GTCTGGACCTGGTGAGTTTCCC <u>CAGGAGCC</u> -MR-3'
<i>CalA1185-1206(-)</i> HICS87	DNA	5'-dMeOAE- <u>CCGAGGAC</u> GTCTGGACCTGGTGAGTTTCCC <u>GTCCTCGG</u> -BHQ2-3'
<i>CalA1174-1217(+)</i>	RNA	3'- <u>GGAUAACA</u> CAGACCUGGACCACUCAAAGG <u>GCACAACUCAG</u> -5'
		<div style="display: flex; justify-content: space-around; width: 100%;"> <span> </span> <span> </span> <span> </span> <span> </span> </div> <div style="display: flex; justify-content: space-around; width: 100%;"> <span>1210</span> <span>1200</span> <span>1190</span> <span>1180</span> </div>
<i>CtrB1452-1465(+)</i> HICS51	OMe	5'-AE- <u>CCGAC</u> AGAGCGAUGAGAAC GUCGG-BHQ2-3'
<i>CtrB1447-1470(-)</i>	OMe	5'- <u>C</u> -3'-3'- <u>AGGCA</u> UCUCGCUACUCUUG CCAAU-5'
		<div style="display: flex; justify-content: space-around; width: 100%;"> <span> </span> <span> </span> <span> </span> </div> <div style="display: flex; justify-content: space-around; width: 100%;"> <span>1450</span> <span>1460</span> <span>1470</span> </div>
<i>NgoA133-145(+)</i> HICS62	OMe	5'-dMeOAE- <u>CCGAG</u> GUACCGGGUAGCG CUCGG-BHQ2-3'
<i>NgoA128-150(-)</i>	OMe	5'- <u>C</u> -3'-3'- <u>CCUUG</u> CAUGGCCCAUCGC CCCC-5'
		<div style="display: flex; justify-content: space-around; width: 100%;"> <span> </span> <span> </span> <span> </span> </div> <div style="display: flex; justify-content: space-around; width: 100%;"> <span>130</span> <span>140</span> <span>150</span> </div>

<sup>a</sup>Names indicating probe sequence ranges corresponding to target sequence ranges are denoted by three letter abbreviations (Genus species) of the reference sequences, a letter indicating whether the small (A) or large (B) rRNA subunit, and the target sequence range (probes have an additional unique designation, e.g., HICS16, from a longer list of previous probes): *Eco*-series sequences<sup>20</sup> are pan-bacterial probes and targets to/from the *Escherichia coli* O157:H7 23S rRNA reference sequence (NCBI accession no. E16366); *Cal*-series sequences<sup>20</sup> are pan-fungal probes and targets to/from the *Candida albicans* 18S rRNA reference sequence (NCBI accession no. E15168); *Ctr*-series sequences are probes and targets to/from TMA amplicon sequences of *Chlamydia trachomatis* 23S rRNA (NCBI accession no. AM884176); *Ngo*-series sequences are probes and targets to/from TMA amplicon sequences of *Neisseria gonorrhoeae* 16S rRNA (NCBI accession no. NC\_002946). Target names are given in bold characters. <sup>b</sup>Nucleic acid backbone sugar structures used for corresponding sequences: DNA, deoxyribose; RNA, ribose; OMe, 2'-O-methylribose (OMe oligonucleotides have similar affinities for complementary RNA sequences<sup>21</sup> while being more resistant to nucleases than RNA oligonucleotides<sup>22</sup>). <sup>c</sup>Underlined probe sequences are composed of DNA, and remaining probe sequences are composed of OMe. <sup>d</sup>AE and dMeOAE are N-linked chemiluminophores introduced using labeling reagent 3 or 4, respectively. BHQ2 and MR are Black Hole Quencher-2 and methyl red quenching moieties, respectively.

their termini to maximize the affinity of the stem arms for each other. The probe sequences were furnished with one of two quenching moieties: (i) a 3'-BHQ2 unit incorporated as part of the oligonucleotide synthesis; (ii) an iodoacetyl-methyl red labeling reagent<sup>9,10</sup> allowed to react with (after reduction) a 3'-disulfide group incorporated as part of the oligonucleotide synthesis. The probe oligonucleotides were synthesized with a terminal protected 5'-hexylamino phosphoramidite at the end of the oligonucleotide synthesis sequence. After deprotection, the chemiluminophore reagents were used to label the freed 5'-NH<sub>2</sub> group. The seven probes produced were purified and quantified prior to use.

**Testing of the Probes.** Substituents on the phenoxide leaving group of an AE have major implications for the rate of the chemiluminescent reaction, but all of our probes had the same leaving group, chosen to provide a balance for initiation of the reaction at moderate pH. However, substituents on the acridinium ring can influence the rate of reaction,<sup>3b</sup> so it was important also to investigate the time courses of emissions and advantageously use differences found to enhance discrimination of emissions. Therefore, several additional characterizations were undertaken, namely, time-resolved spectrography and time-resolved chemiluminescent intensity measurements for individual probes in nonhybridized and fully hybridized forms and

dose-response measurements for both individual probes and mixtures of probes in the presence of a single or two different target oligonucleotides.

**Time-Resolved Spectrography.** In order to understand how 2,7-dimethoxy substitution of the AE changes photonic output compared to the unsubstituted AE, serial emission images were collected at regular time intervals with an SE200 echelle-type (diffraction grating-based) low light, digital spectrograph after chemical initiation of the different HICS probes, transformed to spectrograms and smoothed. As evidenced from the time-resolved spectrograms of the *N*-alkylacridone from probe *EcoB1932-1947(-)*HICS18 hybridized to an equimolar amount of its complementary target (*EcoB1921-1958(+)*, Figure 1a), chemiluminescence increased rapidly in the 400–500 nm range (with smaller contributions from 500–540 nm) during the first 1–1.5 s (compare the initial baseline-level spectrogram at *t* = 0 with the two immediately subsequent spectrograms), followed by a slower decay for at least 15 s (spectrograms 3–23). In the absence of target, chemiluminescence from this probe was low over the entire time course (Figure 1b), similar to the chemiluminescence of the buffer in the absence of probe (data not shown). Double emission maxima at about 425 and 448 nm were readily evident in the *EcoB1932-1947(-)*HICS18 plus target

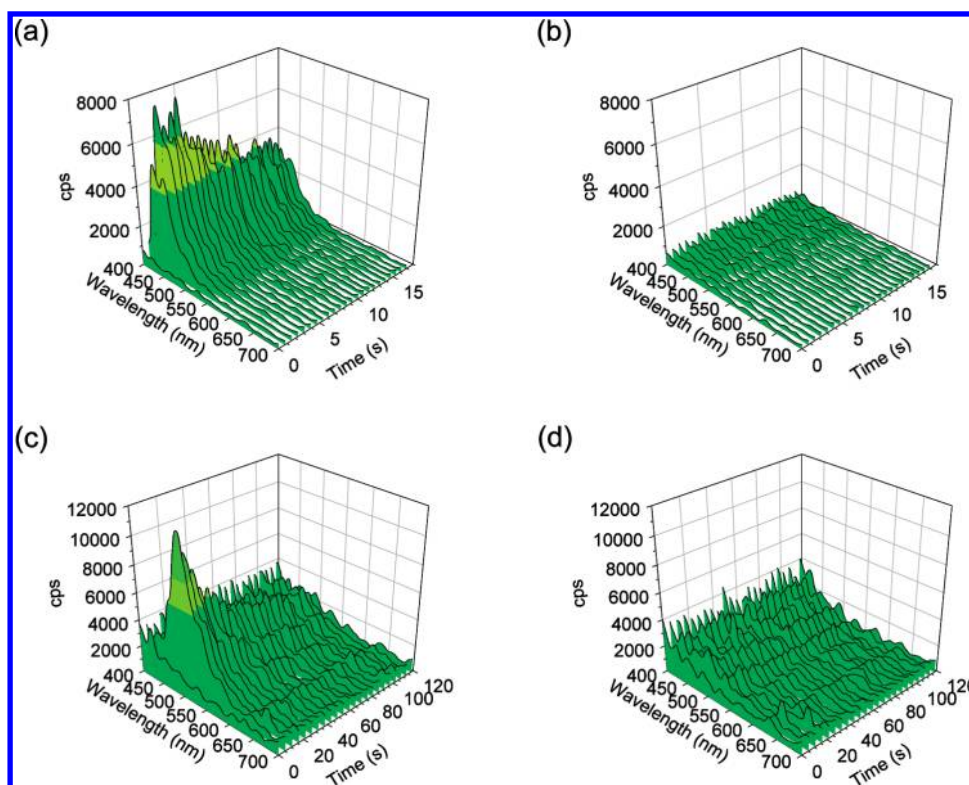


**Figure 1.** Examples of time-resolved spectrograms after chemical initiation: (a) 50 pmol each of *EcoB1932-1947(-)HICS18* and *EcoB1921-1958(+)*; (b) 50 pmol of *EcoB1932-1947(-)HICS18*; (c) 300 pmol each of *CalA1185-1206(-)HICS87* and *CalA1174-1217(+)*; (d) 300 pmol of *CalA1185-1206(-)HICS87*. Curves show the counts per second (cps) summed over the preceding 0.4 s interval (a, b) or the preceding 5 s interval (c, d). Color patterns in graphs are to better distinguish signal magnitudes and consecutive spectrograms.

chemiluminescence spectrograms, consistent with *N*-alkylacridone fluorescence peaks at about 430 and 450 nm that we have observed in water<sup>15c</sup> and peaks at 430 and 443 nm previously reported in aqueous ethanol.<sup>23</sup> The leading edges of the AE spectrograms were steep, while the trailing edges (higher wavelengths) were somewhat broad beyond the second peak. The magnitudes of chemiluminescent spectrograms from the *N*-alkyldimethoxyacridone of probe *CalA1185-1206(-)HICS87* hybridized to an equimolar amount of its complementary target (*CalA1174-1217(+)*, Figure 1c) increased rapidly in the 440–550 nm range {compare the initial spectrogram at  $t = 0$  with the immediately subsequent spectrogram; chemiluminescence from this probe in the absence of target was low over the entire time course (Figure 1d), again comparable to buffer alone (data not shown)}. However, chemiluminescence from the *N*-alkyldimethoxyacridone decayed much more slowly than the *N*-alkylacridone (spectrograms 3–23), nearing background levels after 120 s. Single peak emissions were at  $\sim 483$  nm, very nearly the same as the 485 and 484 nm peaks found for related compounds in water<sup>15</sup> and dimethylformamide,<sup>14</sup> respectively. However, the present results also showed a pronounced shoulder at  $\sim 525$  nm. This shoulder from the *N*-alkyldimethoxyacridone was separated substantially more than the double peaks from the unsubstituted *N*-alkylacridone (about 40 nm versus 23 nm, respectively). The leading and trailing edges of the *N*-alkyldimethoxyacridone were more symmetric than those of *N*-alkylacridone. The emission rise and fall was uniform across spectrograms of both HICS probes, without any isosbestic points, supporting emitted chemiluminescence arising from a

single species. Although partially overlapping, the emissions from these two acridinium esters were substantially separated below  $\sim 450$  nm and above  $\sim 550$  nm. In addition to defining the wavelength ranges expected from probes with these two labels, the spectrography results suggested initial ranges for quantifying time-based constants for the different probes.

**Time-Resolved Chemiluminescence.** Constants for total chemiluminescent emissions from HICS probes were determined after hybridization to excess complementary target oligonucleotides. Preliminary hybridization time courses indicated that incubation for 40 min at 60 °C and 10 min at room temperature was sufficient to maximize signal output from each probe under the conditions employed (data not shown). Plots of counts per second (cps) versus time indicated a rapid increase in emissions to a maximum followed by a slow decrease trending toward the baseline (Figure 2). Background (probe but no target) emissions followed similar time course patterns but with substantially attenuated magnitudes (Figure 2, insets; note the different scales compared to those in the presence of targets).

Multiple series of chemical events occur upon addition of alkaline peroxide to AEs (Scheme S1 in Supporting Information). In order to be able to compare different probes quantitatively, it was necessary to simplify the kinetic scheme for the reactions leading to the increase and decrease in chemiluminescence and then to test this scheme against the observed data. AEs are chemically similar to lucigenin in that both classes of compounds emit light through the same type of chemiluminescent intermediate, an excited *N*-alkylacridone. In the reaction of lucigenin with basic oxygen, Maskiewicz et al. demonstrated that

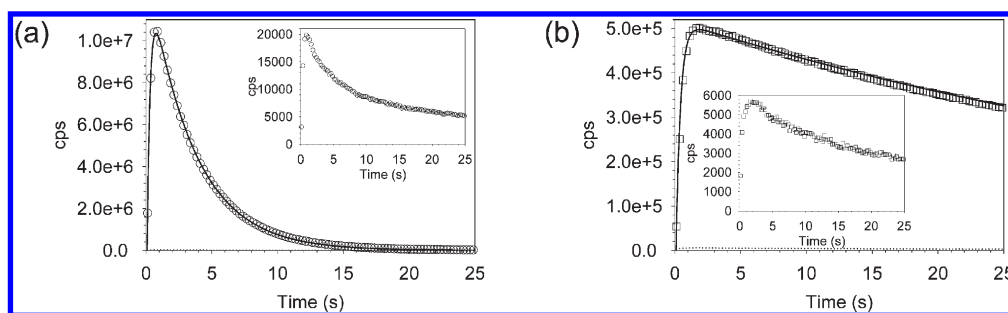


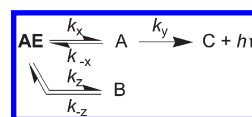
**Figure 2.** Representative time courses of chemiluminescent emissions for (a) 0.5 pmol of *EcoB1932-1947(-)*HICS18 plus 1 pmol of *EcoB1921-1958(+)* and (b) 0.5 pmol of *CalA1185-1206(-)*HICS87 plus 1 pmol of *CalA1174-1217(+)*. Each point shows the cps summed over a 0.25 s interval. Insets are output from 0.5 pmol probes in the absence of target. Lines through data points are nonlinear best fits to a linear combination of exponential functions (eq 1).

despite photon emission from the excited *N*-methylacridone being the result of a minor reaction path, a pair of apparent first-order reactions for the formation and decay of chemiluminescent emissions accounted for their data based on a pair of competing, parallel reactions.<sup>24</sup> We adapted their kinetic scheme of processes discernible by chemiluminescence for our needs (Scheme 3). This scheme only considers rate limiting formation of a preluminescent intermediate A from the AE label prior to initiation of chemiluminescence, rapid formation of a postluminescent product C with emission of light, and a competing reaction to give a nonchemiluminescent product B. If the dark process competes effectively with the process leading to intermediate A, the concentration of A decreases rapidly from its peak and the overall emission process is of short duration. If the dark process is much slower than the process leading to intermediate A, then the emission profile reflects more closely the rate of formation of A and the overall emission process is of longer duration. Data in plots of light emission versus time (e.g., Figure 2) were fitted to a linear combination of exponential functions based on this scheme (eq 1, where *a* and *b* are pre-exponential factors for *k<sub>a</sub>* and *k<sub>b</sub>*, respectively; *k<sub>a</sub>* = *k<sub>x</sub>* − *k<sub>-x</sub>* is the apparent first-order rate constant for the rate determining step for increase in light intensity; *k<sub>b</sub>* = *k<sub>z</sub>* − *k<sub>-z</sub>* is the apparent first-order rate constant for the decrease in light intensity; *k<sub>y</sub>* is the constant for the rapid emission of light as the excited intermediate decays to its ground state; *k<sub>y</sub>* > *k<sub>b</sub>*; and *t* is time in seconds). The constants *k<sub>a</sub>* and *k<sub>b</sub>*, specific activities, and signal-to-background ratios are compared along with other parameters in Table 2.

$$\text{cps} = a(-\exp^{-k_a t}) + b(\exp^{-k_b t}) \quad (1)$$

The emission increase constant (*k<sub>a</sub>* in Scheme 3 and eq 1) varied little more than ~2-fold despite the different probes varying in terms of target-specific sequence, ribose backbone, labels and quenching moieties (Table 2). This is consistent with all of the probes containing the same 2,6-dibromophenoxy leaving group. The constant for decreasing emission (*k<sub>b</sub>*), on the other hand, varied ~125-fold among probes, leading to *τ*<sub>1/2</sub> for decay in light emission ranging from 0.75 to 94 s. However, for a given AE label-quencher combination, *k<sub>b</sub>* varied only up to ~3-fold (e.g., 1.1-fold for probes containing AE and methyl red; 3.2-fold for probes containing AE and BHQ2; and 2.5-fold for probes containing 2,7-dimethoxyAE and BHQ2). The average value of *k<sub>b</sub>* for the two probes bearing a 2,7-dimethoxyAE unit was almost 30 times lower than the average value for all probes bearing an AE unit without modifications at acridinium positions

### Scheme 3. Discernible Reaction Events Supporting Observed Chemiluminescent Emissions from AEs



1–8, indicating that the dark reaction was much less significant for 2,7-dimethoxyAEs than for unmodified AEs. The time to peak, a balance of formation and decay of light emissions, varied ~3.3-fold among the probes. Not surprisingly, the probes with the longest times to peak and smallest *k<sub>b</sub>* values were those comprising 2,7-dimethoxyAE units, which clearly exhibited emission over longer periods of time (Figure 2). Probes bearing unsubstituted AE units and quenchers with a wavelength absorption profile that was well matched with the emitter wavelength profile (e.g., *EcoB1932-1947(-)*HICS16, *CalA1185-1206(-)*HICS86) had longer times-to-peak, smaller values of *k<sub>b</sub>*, and lower *S/B* than the probes for which the quencher absorption profile was less well matched to the emitter profile (e.g., *EcoB1932-1947(-)*HICS17, *EcoB1932-1947(-)*HICS18, *CtrB1452-1465(+)*HICS51). With the exception of the pan-bacterial probe with a methyl red quencher, which showed an SA of only ~4 × 10<sup>7</sup> Σcps/pmol and a *S/B* of less than 5, SA and *S/B* of all probes were high, exceeding 10<sup>8</sup> Σcps/pmol and 40, respectively.

Chemiluminescent emission constants were used to select probe constructs with preferred attributes. For the current studies, the *Ctr/Ngo* pair of distinguishable probes and their target was not chosen as a model system because of the very long data collection that would be required for *NgoA133-145(+)*HICS62 (*Sτ*<sub>1/2</sub> ≈ 7.8 min). The only pan-fungal probe that could be clearly distinguished from the pan-bacterial AE-labeled probes was 2,7-dimethoxyAE-labeled *CalA1185-1206(-)*HICS87. From the pan-bacterial probes, the SA and *S/B* from *EcoB1932-1947(-)*HICS16 were substantially lower than from *EcoB1932-1947(-)*HICS17 or *EcoB1932-1947(-)*HICS18. Preliminary experiments with *EcoB1932-1947(-)*HICS17 and *CalA1185-1206(-)*HICS87 resulted in increased quenching of each other as a function of increased specific probe–target hybrid, suggesting interactions between the arms of these two different probes in the open state (data not shown). Therefore, *EcoB1932-1947(-)*HICS18 and *CalA1185-1206(-)*HICS87 were selected for demonstrating utility for simultaneous detection, discrimination, and quantification of two targets in individual samples.



Table 2. Chemiluminescent Emission Constants for HICS Probes<sup>a</sup>

name	time-to-peak (s)	$k_a$ (s <sup>-1</sup> )	$k_b$ (s <sup>-1</sup> )	SA <sup>b</sup> (Σcps/pmol)	S/B <sup>b</sup>
<i>EcoB1932-1947(-)</i> HICS16	1.3 [16]	2.57 ± 0.14 [18]	0.157 ± 0.004 [16]	(3.93 ± 0.22) × 10 <sup>7</sup> [16]	4.60 ± 0.33 [16]
<i>EcoB1932-1947(-)</i> HICS17	0.63 [16]	4.53 ± 0.15 [18]	0.339 ± 0.019 [16]	(2.08 ± 0.06) × 10 <sup>8</sup> [16]	150 ± 6 [16]
<i>EcoB1932-1947(-)</i> HICS18	0.70 [6]	3.99 ± 0.07 [6]	0.291 ± 0.008 [14]	(3.34 ± 0.09) × 10 <sup>8</sup> [14]	285 ± 10 [14]
<i>CalA1185-1206(-)</i> HICS86	1.0 [18]	3.49 ± 0.17 [20]	0.141 ± 0.003 [18]	(3.74 ± 0.08) × 10 <sup>8</sup> [18]	73.3 ± 2.8 [18]
<i>CalA1185-1206(-)</i> HICS87	1.8 [16]	2.92 ± 0.27 [18]	0.0188 ± 0.0004 [16]	(2.27 ± 0.04) × 10 <sup>8</sup> [2]	93.6 ± 2.5 [2]
<i>CtrB1452-1465(+)</i> HICSS1	0.75 [14]	2.11 ± 0.09 [14]	0.924 ± 0.019 [14]	(1.72 ± 0.04) × 10 <sup>8</sup> [14]	276 ± 11 [14]
<i>NgoA133-145(+)</i> HICS62	2.1 [14]	2.86 ± 0.21 [17]	0.00735 ± 0.00032 [14]	(1.67 ± 0.07) × 10 <sup>8</sup> [3]	40.4 ± 1.8 [3]

<sup>a</sup> Values are the mean ± standard deviations. Numbers in brackets are numbers of replicates.  $k_a$  and  $k_b$  are from nonlinear best fits to eq 1 from at least 5 × first-order half-lives ( $\tau_{1/2}$ ) of each constant. <sup>b</sup> Specific activities (SA) are from the summed cps from  $5\tau_{1/2}$  of the decay process divided by the picomoles of probe, and signal-to-background ratios (S/B) are from the summed cps of  $5\tau_{1/2}$  of the decay process for probe–target hybrids divided by the same sum for probes alone.

*Simultaneous Chemiluminescent Responses from Probes Hybridizing to Target Sequences.* Since the probes were designed, and shown (vide supra), to be distinguishable within a mixture by differences in wavelengths of emission, it was necessary to adapt a luminometer to distinguish multiple wavelengths simultaneously. This was achieved for two probe systems by incorporation of a second PMT into a luminometer and separately attenuating the pair of PMTs with two different filters, one of which allowed light of relatively short wavelength ( $\leq 450$  nm) to pass while the other allowed only light of longer wavelength ( $\geq 550$  nm) to pass.

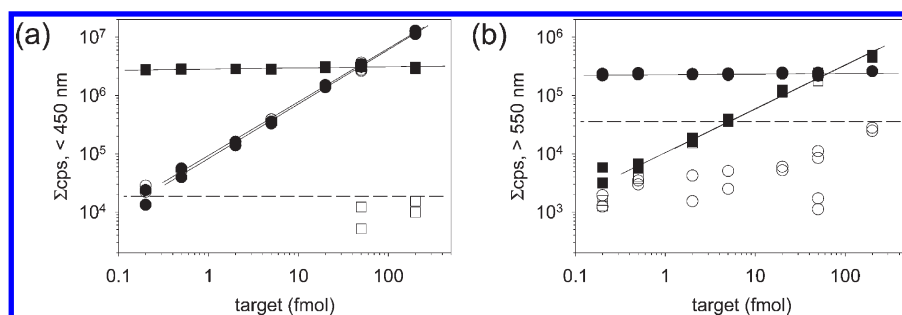
In an attempt to emulate assay conditions for simultaneous, direct detection of bacteria and/or fungi in an environmental sample, constant amounts of both *EcoB1932-1947(-)*HICS18 and *CalA1185-1206(-)*HICS87 were allowed to hybridize to increasing amounts of one, the other, or both target nucleic acids in a mixture of seawater and hybridization reagent. As is evident from Figure 1, some longer wavelength emissions from *EcoB1932-1947(-)*HICS18 overlapped with some shorter wavelength emissions from *CalA1185-1206(-)*HICS87. Such overlaps could be problematic for distinguishing emissions at higher concentrations of each target. However, emission decays from *EcoB1932-1947(-)*HICS18 were rapid after a high peak emission, while those from *CalA1185-1206(-)*HICS87 were considerably slower and had a substantially lower maximum peak intensity (Figure 2 and Table 2). Taking advantage of wavelength separations as well as these timing differences facilitated considerable reduction in overlapping emissions from these probes at high concentrations without detrimental reduction in specific target signal intensities.

Figure 3 demonstrates spectral–temporal resolved emissions from one example of several target dilutions. The deconvoluted response from *EcoB1932-1947(-)*HICS18 (corresponding to the first 12 s of emission measured at  $\leq 450$  nm, Figure 3a) was linearly quantitative from 500 amol to 200 fmol of bacterial nucleic acid *EcoB1921-1958(+)* in the absence or presence of a high concentration (50 fmol) of fungal *CalA1174-1217(+)*; *EcoB1921-1958(+)* curves in the absence or presence of *CalA1174-1217(+)* are nearly indistinguishable except at the lowest target concentrations. As evidenced by the near zero slope ( $m < 0.02$ ) of the line linking emissions from solutions containing 50 fmol of bacterial target and various amounts of fungal target, the presence of fungal target (200 amol to 200 fmol) did not appreciably influence the emission responses of *EcoB1932-1947(-)*HICS18 from bacterial target. The deconvoluted response from *CalA1185-1206(-)*HICS87 (corresponding to the

emission measured at  $\geq 550$  nm between 12 and 184 s, Figure 3b) was also linearly quantitative from  $\sim 500$  amol to 200 fmol of fungal target in the absence or presence of a high concentration (50 fmol) of bacterial target; *CalA1174-1217(+)* curves in the absence or presence of *EcoB1921-1958(+)* are nearly indistinguishable except at the lowest target concentrations. Very high concentrations (e.g., 200 fmol) of bacterial target in the absence of fungal target yielded substantial long wavelength and long-lived emissions, effectively limiting the quantitative detection range of *CalA1185-1206(-)*HICS87 in the presence of possible bacterial target to just over 5 fmol to 200 fmol. Similar to *EcoB1932-1947(-)*HICS18, the emission responses from *CalA1185-1206(-)*HICS87 plus 50 fmol fungal target were minimally influenced by the presence of 200 amol to 200 fmol bacterial target ( $m < 0.02$ ). The slopes and intercepts of the specific target dilutions were similar to each other in the absence or presence of the other target, and repeated experiments demonstrated similar results (Table S1 in Supporting Information).

From a single analyte point of view, the current results are close to or exceed the sensitivity reported in many literature examples. For example, in a heterogeneous, single-analyte, sandwich-type antibody assay with eight complex 2,7-di-alkoxyAE labels (similar relative quantum yields as 2,7-dimethoxyAE) per secondary antibody, as little as 28 pmol of theophylline could be detected.<sup>14</sup> In a homogeneous, single-analyte molecular assay with a single C-linked AE label per linear DNA probe, 30 amol of *Ctr* target could be detected.<sup>25</sup> Finally, in another molecular assay in which single analytes were captured on magnetic particles in a ternary complex conjugated to horseradish peroxidase, chemiluminescent detection of DNA target was down to 10 amol.<sup>26</sup> However, compared with such tests, the present method has the major advantage of being suitable for simultaneous measurement of two analytes.

Other label and detection strategies have been used to quantify multiple analytes in individual, nonamplified samples. For example, Adamczyk et al. captured bovine serum albumin and myoglobin from a common solution, removed unbound materials by washing, and detected 100 fmol to 100 pmol of the analytes in the same solution by sequentially triggering aequorin label with Ca<sup>2+</sup>, recording luminescence, then triggering an AE label with alkaline peroxide and recording luminescence.<sup>27</sup> Using acridinium- and benz[*b*]acridinium-labeled antibodies to follicle-stimulating hormone (FSH) and luteinizing hormone (LH), respectively, in a heterogeneous



**Figure 3.** Spectral–temporal deconvolution of chemiluminescent emissions due to *EcoB1932-1947(-)*-HICS18 and *CalA1185-1206(-)*-HICS87 from mixtures containing 200 fmol of both probes plus various amounts of target (calibration curves) in a 1:1 mixture of seawater and 2× hybridization reagent. Open symbols are for *EcoB1921-1958(+)* (○) or *CalA1174-1217(+)* (□) alone, while closed symbols are for *EcoB1921-1958(+)* (●) or *CalA1174-1217(+)* (■) plus 50 fmol of the other target. (a) Each point shows the wavelength-resolved cps (<450 nm) summed over  $5t_{1/2}$  of *EcoB1932-1947(-)*-HICS18 (0–12.0 s). (b) Each point shows the wavelength-resolved cps (>550 nm) summed from the end of the first  $5t_{1/2}$  of *EcoB1932-1947(-)*-HICS18 to the end of the first  $5t_{1/2}$  of *CalA1185-1206(-)*-HICS87 (12.0–184 s). All conditions were performed in at least duplicate. Lines through background-subtracted data points are linear best fits (Table S1). The intersections of the solid target-response and dashed lines indicate the minimum of one target that can be distinguished in the presence of a high quantity (200 fmol) of the other target.

assay, Law et al. disclosed dual, wavelength-resolved detection of FSH and LH down to about 10–20 mIU/mL over about 10- and 5-fold concentration ranges.<sup>13</sup> Nelson et al. used pairs of linear nucleic acid probes labeled with *N*-methyl AE that differed in the  $pK_a$  of their phenolic leaving groups and, hence, in their emission time constants to homogeneously detect and quantify by time resolution as little as 500 amol of *NgO* or 150 amol of *Ctr* over a 20-fold concentration range in the absence or presence of the other analyte.<sup>3b</sup> While this last example demonstrated higher sensitivity for one of a pair of dual analytes, the dynamic range for the other analyte was narrower than in the current study (e.g., Figure 3).

## CONCLUSIONS

A new chemiluminescent label incorporating a 2,7-dimethoxy-AE unit has been synthesized and used to generate HICS probes. Emission constants of these probes have been characterized and compared to an existing HICS probe label design. Unimodal rise-and-decay of spectrograms over time from both probe types supports that emissions are from the generation of excited acridone species from AE- and from 2,7-dimethoxyAE-labeled probes. Peak emissions from 2,7-dimethoxyAE-labeled probes shift bathochromatically by ~58 nm from those of AE-labeled probes. Time-resolved chemiluminescent emissions indicate that 2,7-dimethoxyAE-labeled probes have emitter formation rates that are similar to those from AE-labeled probes but that they have substantially slower emission decay rates because of slower dark reactions of the AE. These differences in emission wavelengths and time courses advantageously support simultaneous spectral–temporal separation of signals from two probes in a dual wavelength luminometer. This allowed demonstration of a rapid (~60 min/sample), sensitive (about 500 amol to 5 fmol), and homogeneous detection and quantification (dynamic range spanning up to 3 log concentration units) process without enzymatic amplification of two microbial target nucleic acids representing those that may be present in single environmental samples. In principle, the method lends itself to providing further assay value by addition of extra detection channels to the luminometer and by including one or more additional spectrally and temporally resolved probes to other analytes or internal controls.

## EXPERIMENTAL SECTION

**(1) Organic Synthesis.** (1.a) *General.* Chemicals and reagents were obtained from Aldrich Chemical Co. and were used without further purification unless otherwise stated. Tetrahydrofuran (THF) was distilled from sodium benzophenone ketyl. Other solvents were purified by standard procedures.<sup>28</sup> Melting point determinations were performed by the open capillary method using a Gallenkamp melting point apparatus and are reported uncorrected. <sup>1</sup>H and <sup>13</sup>C NMR spectra were recorded on an AV500 spectrometer operating at 500 MHz for <sup>1</sup>H or 125 MHz for <sup>13</sup>C measurements. Chemical shifts  $\delta$  are reported in parts per million (ppm) relative to tetramethylsilane, and coupling constants *J* are in Hz. Low- and high-resolution mass spectra were recorded on a GCT-Premier spectrometer, electron impact (EI) at 70 eV. Atmospheric pressure chemical ionization (APCI) mass spectra were acquired on a Waters LCT Premier XE instrument. Electrospray (ES) mass spectrometric analyses were performed on a ZQ4000 instrument in positive ionization mode. Column chromatography was carried out using Fisher Scientific silica 60A (35–70  $\mu$ m).

(1.b) *Bis(4-methoxyphenyl)amine (5).* Compound 5 was prepared in 75% yield according to a standard literature procedure:<sup>16</sup> mp 102–103 °C (lit. 102–103 °C,<sup>29</sup> 99.5–101.5 °C<sup>30</sup>).

(1.c) *N-(4-Methoxyphenyl)-5-methoxyisatin (6).* A solution of 5 (3.21 g, 14.0 mmol) in dichloromethane (CH<sub>2</sub>Cl<sub>2</sub>, 40 mL) was added dropwise to a stirred, refluxing solution of oxalyl chloride (3.53 g, 28.0 mmol) in CH<sub>2</sub>Cl<sub>2</sub> (70 mL). The mixture was heated under reflux for 1 h, and the excess oxalyl chloride and CH<sub>2</sub>Cl<sub>2</sub> were then removed under reduced pressure. To the residue, CH<sub>2</sub>Cl<sub>2</sub> (100 mL) was added, followed by anhydrous AlCl<sub>3</sub> (4.32 g, 32.4 mmol) portionwise over 10 min. The mixture was heated under reflux for 1 h. The solvent was removed under reduced pressure, and to the residue was added dilute HCl (40 mL of ~1 M). The mixture was stirred for 30 min and was then extracted with CHCl<sub>3</sub> (3 × 30 mL). The extracts were combined and dried (MgSO<sub>4</sub>), and the solvent was removed under reduced pressure. The solid obtained was washed with CH<sub>2</sub>Cl<sub>2</sub> to give pure 6 (2.78 g, 9.81 mmol; 70%): mp 203–205 °C; <sup>1</sup>H NMR (CDCl<sub>3</sub>)  $\delta$  7.34 (d, *J* = 9.0 Hz, 2H), 7.25 (d, *J* = 2.8 Hz, 1H), 7.13 (dd, *J* = 2.8 and 8.6 Hz, 1H), 7.07 (d, *J* = 9.0 Hz, 2H), 6.79 (d, *J* = 8.6 Hz, 1H), 3.88 (s, 3H), 3.84 (s, 3H); <sup>13</sup>C NMR (CDCl<sub>3</sub>)  $\delta$  183.5, 159.5, 157.7, 156.7, 146.1, 127.3, 125.5, 125.0, 117.8, 115.2, 112.3, 109.1, 56.0, 55.6; HRMS (APCI) calcd for C<sub>16</sub>H<sub>14</sub>NO<sub>4</sub> (MH<sup>+</sup>) 284.0923, found 284.0935.

(1.d) *2,7-Dimethoxyacridine-9-carboxylic Acid (7).* A mixture of 6 (1.42 g, 5.00 mmol) and KOH (7.00 g, 125 mmol) in water (70 mL) was

refluxed for 72 h. The resulting mixture, after cooling, was poured into a mixture of concentrated HCl (15 mL) and ice (30 g). The yellow solid obtained was collected by filtration, washed with water and  $\text{CH}_2\text{Cl}_2$ , and then dried in a vacuum oven at 60 °C overnight to give **7** (1.35 g, 4.76 mmol; 95%): mp 192–193 °C;  $^1\text{H}$  NMR ( $\text{DMSO}-d_6$ )  $\delta$  8.32 (d,  $J$  = 9.4 Hz, 2H), 7.75 (dd,  $J$  = 2.6 and 9.4 Hz, 2H), 7.29 (d,  $J$  = 2.6 Hz, 2H), 3.97 (s, 6H). The material was highly insoluble in solvents, and the  $^{13}\text{C}$  NMR spectrum was not recorded. HRMS (EI) calcd for  $\text{C}_{16}\text{H}_{13}\text{NO}_4$  ( $\text{M}^+$ ) 283.0845, found 283.0845.

(1.e) *2,6-Dibromophenyl 2,7-Dimethoxyacridine-9-carboxylate (8)*. A mixture of **7** (1.21 g, 4.27 mmol) and freshly distilled thionyl chloride (20 mL, 69 mmol) was refluxed under anhydrous conditions for 3 h. The excess thionyl chloride was removed under reduced pressure to leave an orange solid. 2,6-Dibromophenol (1.33 g, 5.30 mmol) was dissolved in pyridine (20 mL) by heating at 70 °C, cooled, and transferred into the flask containing the acid chloride. The mixture was heated at 70 °C overnight. The solvent was removed under reduced pressure, and the residue obtained was extracted with  $\text{CH}_2\text{Cl}_2$ . The extract was concentrated, and the residue obtained was purified by column chromatography (silica gel;  $\text{Et}_2\text{O}$ –hexane, 1:3) to give **8** (1.48 g, 2.86 mmol; 67% yield): mp 245–247 °C;  $^1\text{H}$  NMR ( $\text{CDCl}_3$ )  $\delta$  8.17 (d,  $J$  = 9.4 Hz, 2H), 7.89 (d,  $J$  = 2.6 Hz, 2H), 7.74 (d,  $J$  = 8.1 Hz, 2H), 7.48 (dd,  $J$  = 2.6 and 9.4 Hz, 2H), 7.18 (t,  $J$  = 8.1 Hz, 1H), 4.02 (s, 6H);  $^{13}\text{C}$  NMR ( $\text{CDCl}_3$ )  $\delta$  164.0, 158.9, 146.7, 144.25, 132.9, 131.8, 128.9, 128.2, 125.0, 124.3, 117.9, 101.3, 56.1; HRMS (EI) calcd for  $\text{C}_{22}\text{H}_{15}\text{NO}_4^{79}\text{Br}_2$  ( $\text{M}^+$ ) 514.9368, found 514.9367.

(1.f) *Succinimidyl 4-Iodobutanoate*. Succinimidyl 4-iodobutanoate was prepared in 84% yield according to a standard literature procedure:<sup>10</sup> mp 86–87 °C (lit. 86–87 °C<sup>10</sup>).

(1.g) *9-(2,6-Dibromophenoxyacarbonyl)-2,7-dimethoxy-10-(3-succinimidylloxycarbonylpropyl)acridinium Iodide (4)*. A well-mixed mixture of **8** (50 mg, 0.091 mmol) and succinimidyl 4-iodobutanoate (50 mg, 0.16 mmol) was heated in an oil bath (150 °C) for 3 h under nitrogen. The mixture turned to dark brown, and acetonitrile (3 × 1 mL) was used to extract the product. The crude product was precipitated with diethyl ether (10 mL), then subjected to extensive washing with diethyl ether and diethyl ether/ $\text{CH}_2\text{Cl}_2$  mixture (5/1 by volume) until TLC showed that all the starting materials were removed, leaving **4** as a brownish solid (3 mg, 0.0036 mmol; 4%). The washings were evaporated under reduced pressure. The residue was subjected to the same reaction procedure again to give further **4** (1 mg), and the cycle was repeated yet again to give further **4** (1 mg). The total yield of **4** was 6.6%: mp 159–162 °C;  $^1\text{H}$  NMR ( $\text{CD}_3\text{CN}$ )  $\delta$  8.64 (d,  $J$  = 9.5 Hz, 2H), 8.07 (dd,  $J$  = 2.7 and 9.5 Hz, 2H), 7.98 (d,  $J$  = 2.7 Hz, 2H), 7.90 (d,  $J$  = 8.2 Hz, 2H), 7.36 (t,  $J$  = 8.2 Hz, 1H), 5.44 (t,  $J$  = 7.0 Hz, 2H), 4.08 (s, 6H), 3.16 (t,  $J$  = 7.0 Hz, 2H), 2.85 (s, 4H), 2.57 (m, 2H); HRMS ( $\text{ES}^+$ ) calcd for  $\text{C}_{30}\text{H}_{25}\text{N}_2\text{O}_8^{79}\text{Br}_2$  ( $[\text{M} - \text{I}]^+$ ) 698.9978, found 698.9982.

(2) *Oligonucleotides*. (2.a) *Synthesis*. Oligonucleotides were synthesized in-house using an Expedite model 8909 nucleic acid synthesis system {PerSeptive Biosystems (now part of Life Technologies Corporation, Carlsbad, CA)}. The syntheses of the probe oligonucleotides utilized substituted 500 Å controlled pore glass (CPG) substrates packed in automated synthesizer columns. Deoxy CPG were used for RNA target syntheses, resulting in 3'-deoxyribonucleotides on these oligonucleotides. Probe sequences incorporating a 3'-terminal BHQ2 unit started with Black Hole Quencher-2 attached to CPG via a glycolate linker and with a dimethoxytrityl (DMT) protecting the terminal hydroxyl (part no. CG5-5042G, Biosearch Technologies, Inc., Novato, CA), and sequences destined for eventual conjugation to 2-(4-dimethylaminophenylazo)-*N*-[2-(2-iodoacetyl-amino)ethyl]-benzamide (iodoacetyl-methyl red) to incorporate the quenching agent started with 1-*O*-dimethoxytrityl-propyl-disulfide, 1'-succinyl-[long chain alkylamino]-CPG (part no. 20-2933, Glen Research, Sterling, VA). 6-(4-Monomethoxytritylamino)hexyl (2-cyanoethyl)

(*N,N*-diisopropyl) phosphoramidite (part no. 10-1906, Glen Research, Sterling, VA) was used to functionalize probe oligonucleotides with 5'-terminal amine linker arms. The dimethoxytrityl group was removed (as trityl groups were for subsequently incorporated phosphoramidites) by machine-automated detritylation with trichloroacetic acid in dichloromethane according to vendor recommendations. After completion of their syntheses, oligonucleotides were cleaved from the CPG column under standard conditions with ammonium hydroxide, followed by purification by standard polyacrylamide gel electrophoretic separation as previously described.<sup>4</sup>

(2.b) *Labeling of the Oligonucleotides*. The oligonucleotides were deprotected to liberate the terminal amino group according to vendor recommendations. The amino groups were then labeled through the succinimidyl groups of 9-(2,6-dibromophenoxyacarbonyl)-10-(3-succinimidylloxycarbonylpropyl)acridinium iodide (**3**)<sup>9,10</sup> or 9-(2,6-dibromophenoxyacarbonyl)-2,7-dimethoxy-10-(3-succinimidylloxycarbonylpropyl)acridinium iodide (**4**).<sup>10</sup> The 3'-disulfides were reduced according to vendor recommendation ([http://www.glenresearch.com//Technical/TB\\_Thiol\\_Modifier\\_S-S.pdf](http://www.glenresearch.com//Technical/TB_Thiol_Modifier_S-S.pdf), accessed Nov 3, 2010) with dithiothreitol and coupled with iodoacetyl-methyl red<sup>9</sup> according to the literature procedure.<sup>9,10</sup> The fully labeled oligonucleotides were purified by reversed phase HPLC as previously described.<sup>4</sup> The structures of the oligonucleotides (labeled or not) were confirmed by MALDI-TOF MS (Supporting Information), and their concentrations were determined by conventional absorption spectroscopy using a DU 640B spectrophotometer (Beckman Coulter, Inc., Brea, CA).

(2.c) *Chemiluminescent Spectrographic Emissions*. Time-resolved, spectrographic images of HICS probe chemiluminescent emissions were acquired on a low light, echelle-type SE200 spectrograph (Optomechanics Research Inc., Vail, AZ) using KestrelSpec software (Catalina Scientific Corp., Tucson, AZ). The images were converted to spectrograms at 1 nm resolution and then smoothed (4%) with a locally weighted scatter plot smoothing algorithm<sup>31</sup> (Excel Add-In, Peltier Technical Services, <http://peltiertech.com/>, accessed Jul 31, 2009). An amount of 50 pmol/100  $\mu\text{L}$  of AE-bearing probes (Table 1) or 300 pmol/100  $\mu\text{L}$  of 2,7-dimethoxyAE-linked probes (Table 1), either alone or together with 50 or 300 pmol/100  $\mu\text{L}$  of the corresponding specific synthetic target (Table 1), was allowed to incubate for 15 min at 60 °C in a low pH, surfactant-containing 1 × hybridization reagent (indicating hybridization or predetection concentrations; 95 mM succinic acid, 1.5 mM ethylenediamine-*N,N,N',N'*-tetraacetic acid, 1.5 mM ethylene glycol-bis(2-aminoethylether)-*N,N,N',N'*-tetraacetic acid, 312 mM lithium dodecyl sulfate, 125 mM LiOH, pH 5.2)<sup>9</sup> and cooled for at least 15 min at room temperature. These conditions allowed probe loop hybridization to target sequences to occur in the solutions containing target and probe stem hybridization to occur in solutions without target. Chemiluminescence from 100  $\mu\text{L}$  of each of the solutions (probes incubated with or without complementary target) was initiated by a single 100  $\mu\text{L}$  injection of 240 mM  $\text{H}_2\text{O}_2$ /2 M Tris-HCl, pH 9.0, solution, and data collection was started immediately (for 25 × 0.4 s or 5 s intervals separated by 0.37 s pauses for the AE-linked or 2,7-dimethoxyAE-linked probes, respectively).

(2.d) *Chemiluminescent Constants*. Chemiluminescent emission time courses were acquired on a Gen-Probe Incorporated LEADER HC+ luminometer. Solutions containing 0.5 pmol/100  $\mu\text{L}$  probe with or without 1 pmol/100  $\mu\text{L}$  specific synthetic target in 1 × hybridization reagent plus 100  $\mu\text{L}$  of silicone oil were mixed by vortexing in 12 mm × 75 mm polypropylene tubes and allowed to incubate in a 60 °C water bath for 40 min to facilitate hybridization of probes and targets (when present). After the mixtures had cooled to room temperature for at least 10 min, chemiluminescent emissions were initiated by a 200  $\mu\text{L}$  injection of detect 1 solution (240 mM  $\text{H}_2\text{O}_2$ /1 mM  $\text{HNO}_3$ ) followed by a 2 s pause and then a 200  $\mu\text{L}$



injection of detect 2 solution (2 M Tris-HCl, pH 9.0), and data collection was started after the first 40 ms mixing time and continued for at least  $5\tau_{1/2}$  of the apparent first order rate constant  $k_b$  (10–500 s total) without interinterval delays. Final pH after detection was always 9.0. Constants were calculated as described in the Results and Discussion. Interpretation of the kinetic constant  $k_a$  may be limited by the hardware and firmware configurations of the luminometer.

(2.e) *Competitive Wavelength-Resolved Chemiluminescence*. Chemiluminescent emission time courses from 0.2 pmol/100  $\mu$ L of both EcoB1932-1947(-)HICS18 and CalA1185-1206(-)HICS87 probes in hybridization reagent were acquired simultaneously on a luminometer modified for dual wavelength-range detection. This luminometer was equipped with two high-count PMT modules (28 mm diameter, head-on, bialkali cathode, peak cathode radiant sensitivity at 420 nm; Hamamatsu Photonics, Hamamatsu City, Japan) on opposite sides of and directed toward a light-tight detection chamber fitted with injector tubing from two reagent pumps. Filters {25.4 mm diameter; 417/60 BrightLine bandpass filter (transmits  $\sim$ 95% of light from 385 to 450 nm) from Semrock, Inc. (Rochester, NY) for AE, and OG550 cut-on filter (transmits  $\sim$ 90% of light from 550 to 700 nm) from Newport Corporation (Irvine, CA) for 2,7-dimethoxyAE} were fitted between PMT 1 and PMT 2, respectively, and the detection chamber. Custom VisualBasic software controlled reagent injections and chemiluminescent data acquisition from the two PMT channels. Hybridizations were performed substantially as for Chemiluminescent Constants (above) except an amount of 50  $\mu$ L of 0 or 200 amol to 200 fmol/50  $\mu$ L targets in seawater (0.2  $\mu$ m filtered; Scripps Institution of Oceanography Pier, La Jolla, CA) was mixed with 50  $\mu$ L of  $2\times$  hybridization reagent containing 0.5 pmol/50  $\mu$ L of both probes. Chemiluminescence was initiated by a 200  $\mu$ L injection of detect 1 solution followed by a 2 s pause, then a 200  $\mu$ L injection of detect 2 solution, and data collection was started immediately from the dual wavelength luminometer for  $230 \times 0.8$  s intervals (184 s total) without interinterval delays. Final pH after detection was always 9.0.

## ■ ASSOCIATED CONTENT

**S Supporting Information.** AE reaction scheme and table of linear fit constants and additional experimental details. This material is available free of charge via the Internet at <http://pubs.acs.org>.

## ■ AUTHOR INFORMATION

### Corresponding Author

Ken.Browne@gen-probe.com

### Present Address

<sup>†</sup>School of Medicine, Cardiff University, Tenovus Building, Heath Park, Cardiff, Wales CF14 4XN, U.K.

## ■ ACKNOWLEDGMENT

M. Majlessi, the Oligonucleotide Synthesis Group, A. Maheson, and T. Luo at Gen-Probe Incorporated have our gratitude for their syntheses and MS analyses of the nucleic acid constructs presented in this article. We are also indebted to R. Pacheco for assistance designing the dual wavelength luminometer and writing custom data acquisition software. In addition, we thank Molecular Light Technology Research Limited for supplying 9-(2,6-dibromophenoxycarbonyl)-10-(3-succinimidylloxycarbonylpropyl)acridinium iodide and 2-(4-dimethylaminophenylazo)-N-[2-(2-iodoacetyl-amino)ethyl]benzamide. The results of this project are partially based upon work supported by the Air Force Office of

Scientific Research (AFOSR) under Award No. FA9550-07-1-0027 to D.D.D.

## ■ REFERENCES

- (1) (a) Meller, A.; Nivon, L.; Brandin, E.; Golovchenko, J.; Branton, D. *Proc. Natl. Acad. Sci. U.S.A.* **2000**, *97*, 1079–1084. (b) Shendure, J.; Porreca, G. J.; Reppas, N. B.; Lin, X.; McCutcheon, J. P.; Rosenbaum, A. M.; Wang, M. D.; Zhang, K.; Mitra, R. D.; Church, G. M. *Science* **2005**, *309*, 1728–1732. (c) Oszolak, F.; Platt, A. R.; Jones, D. R.; Reifenger, J. G.; Sass, L. E.; McInerney, P.; Thompson, J. F.; Bowers, J.; Jarosz, M.; Milos, P. M. *Nature* **2009**, *461*, 814–818.
- (2) (a) Southern, E. M. *J. Mol. Biol.* **1975**, *98*, 503–517. (b) Fulton, R. J.; McDade, R. L.; Smith, P. L.; Kienker, L. J.; Kettman, J. R., Jr. *Clin. Chem.* **1997**, *43*, 1749–1756. (c) Gunderson, K. L.; Steemers, F. J.; Lee, G.; Mendoza, L. G.; Chee, M. S. *Nat. Genet.* **2005**, *37*, 549–554.
- (3) (a) Tyagi, S.; Kramer, F. R. *Nat. Biotechnol.* **1996**, *14*, 303–308. (b) Nelson, N. C.; Cheikh, A. B.; Matsuda, E.; Becker, M. M. *Biochemistry* **1996**, *35*, 8429–8438. (c) Gaylord, B. S.; Heeger, A. J.; Bazan, G. C. *Proc. Natl. Acad. Sci. U.S.A.* **2002**, *99*, 10954–10957. (d) Storhoff, J. J.; Lucas, A. D.; Garimella, V.; Bao, Y. P.; Müller, U. R. *Nat. Biotechnol.* **2004**, *22*, 883–887.
- (4) Browne, K. A. *J. Am. Chem. Soc.* **2005**, *127*, 1989–1994.
- (5) Becker, M. M.; Schroth, G. P. U.S. Patent 6,534,274, 2003.
- (6) Saiki, R. K.; Gelfand, D. H.; Stoffel, S.; Scharf, S. J.; Higuchi, R.; Horn, G. T.; Mullis, K. B.; Erlich, H. A. *Science* **1988**, *239*, 487–491.
- (7) Brentano, S. T.; McDonough, S. H. *Nonradioactive Analysis of Biomolecules*; Kessler, C., Ed.; Springer-Verlag: New York, 2000; pp 374–380.
- (8) Nelson, N. C.; Reynolds, M. A.; Arnold, L. J., Jr. *Nonisotopic Probing, Blotting, and Sequencing*; Kricka, L. J., Ed.; Academic Press: San Diego, CA, 1995; pp 391–428.
- (9) (a) Rutter, A. J.; Weeks, I.; Li, Z.; Smith, K. U.S. Patent 7,169,554, 2007. (b) Weeks, I.; Rutter, A. J.; Li, Z.; Smith, K. U.S. Patent Application 10/570,175, 2007.
- (10) Brown, R. C.; Li, Z.; Rutter, A. J.; Mu, X.; Weeks, O. H.; Smith, K.; Weeks, I. *Org. Biomol. Chem.* **2009**, *7*, 386–394.
- (11) Campbell, A. K.; Woodhead, J. S.; Weeks, I. U.S. Patent 4,946,958, 1990.
- (12) Woodhead, J. S.; Weeks, I.; Batmanghelich, S. U.S. Patent 5,656,207, 1997.
- (13) Law, S.-J.; Jiang, Q.; Fischer, W.; Unger, J. T.; Krodell, E. K.; Xi, J. U.S. Patent 5,879,894, 1999.
- (14) Natrajan, A.; Sharpe, D.; Costello, J.; Jiang, Q. *Anal. Biochem.* **2010**, *406*, 204–213.
- (15) (a) Batmanghelich, S.; Woodhead, J. S.; Smith, K.; Weeks, I. *J. Photochem. Photobiol., A* **1991**, *56*, 249–254. (b) Batmanghelich, S.; Brown, R. C.; Woodhead, J. S.; Smith, K.; Weeks, I. *J. Photochem. Photobiol., B* **1992**, *12*, 193–201. (c) Smith, K.; Yang, J.-J.; Weeks, I.; Woodhead, J. S. *J. Photochem. Photobiol., A* **2000**, *132*, 181–191. (d) Smith, K.; Yang, J.-J.; Li, Z.; Weeks, I.; Woodhead, J. S. *J. Photochem. Photobiol., A* **2009**, *203*, 72–79. (e) Li, Z. Ph.D. Thesis, University of Wales, Swansea, U.K., 1998.
- (16) Zhang, H.; Cai, Q.; Ma, D. *J. Org. Chem.* **2005**, *70*, 5164–5173.
- (17) (a) Hartz, A.; Cuvelier, M.; Nowosielski, K.; Bonilla, T. D.; Green, M.; Esiobu, N.; McCorquodale, D. S.; Rogerson, A. *J. Environ. Qual.* **2008**, *37*, 898–905. (b) Papadakis, J. A.; Mavridou, A.; Richardson, S. C.; Lampiri, M.; Marcelou, U. *Water Res.* **1997**, *31*, 799–804.
- (18) Johnson, S. J.; Green, D. H.; Reed, D. A.; Wood, L. S. *Clin. Chem.* **2001**, *47*, 760–763.
- (19) Hogan, J. J.; Smith, R. D.; Kop, J. A.; McDonough, S. H. U.S. Patent 5,693,468, 1997.
- (20) Hogan, J. J. U.S. Patent 6,821,770, 2004.
- (21) Lesnik, E. A.; Freier, S. M. *Biochemistry* **1998**, *37*, 6991–6997.
- (22) Sproat, B. S.; Lamond, A. I.; Beijer, B.; Neuner, P.; Ryder, U. *Nucleic Acids Res.* **1989**, *17*, 3373–3386.
- (23) McCapra, F.; Richardson, D. G.; Chang, Y. C. *Photochem. Photobiol.* **1965**, *4*, 1111–1121.



- (24) Maskiewicz, R.; Sogah, D.; Bruce, T. C. *J. Am. Chem. Soc.* **1979**, *101*, 5355–5364.
- (25) Arnold, L. J., Jr.; Hammond, P. W.; Wiese, W. A.; Nelson, N. C. *Clin. Chem.* **1989**, *35*, 1588–1594.
- (26) Cai, S.; Lau, C.; Lu, J. *Anal. Chem.* **2010**, *82*, 7178–7184.
- (27) Adamczyk, M.; Moore, J. A.; Shreder, K. *Bioorg. Med. Chem. Lett.* **2002**, *12*, 395–398.
- (28) (a) Vogel, A. I. *Vogel's Textbook of Practical Organic Chemistry*, 5th ed.; Longman: Harlow, U.K., 1989. (b) Perrin, D. D.; Armarego, W. L. F. *Purification of Laboratory Chemicals*, 3rd ed.; Pergamon Press: Oxford, U.K., 1988.
- (29) McNulty, J.; Cheekoori, S.; Bender, T. P.; Coggan, J. A. *Eur. J. Org. Chem.* **2007**, 1423–1428.
- (30) Wolfe, J. P.; Timori, J.; Sadighi, J. P.; Yin, J.; Buchwald, S. L. *J. Org. Chem.* **2000**, *65*, 1158–1174.
- (31) (a) Cleveland, W. S. *J. Am. Stat. Assoc.* **1979**, *74*, 829–836. (b) Cleveland, W. S.; Devlin, S. J. *J. Am. Stat. Assoc.* **1988**, *83*, 596–610.